

Use of the Parallax-Quench Method to Determine the Position of the Active-Site Loop of Cholesterol Oxidase in Lipid Bilayers[†]

Xiaoyu Chen,[‡] David E. Wolfgang,[‡] and Nicole S. Sampson*

Department of Chemistry, State University of New York, Stony Brook, New York 11794-3400

Received June 20, 2000; Revised Manuscript Received August 25, 2000

ABSTRACT: To elucidate the cholesterol oxidase–membrane bilayer interaction, a cysteine was introduced into the active site lid at position-81 using the *Brevibacterium* enzyme. To eliminate the possibility of labeling native cysteine, the single cysteine in the wild-type enzyme was mutated to a serine without any change in activity. The loop-cysteine mutant was then labeled with acrylodan, an environment-sensitive fluorescence probe. The fluorescence increased and blue-shifted upon binding to lipid vesicles, consistent with a change into a more hydrophobic, i.e., lipid, environment. This acrylodan-labeled cholesterol oxidase was used to explore the pH, ionic strength, and headgroup dependence of binding. Between pH 6 and 10, there was no significant change in binding affinity. Incorporation of anionic lipids (phosphatidylserine) into the vesicles did not increase the binding affinity nor did altering the ionic strength. These experiments suggested that the interactions are primarily driven by hydrophobic effects not ionic effects. Using vesicles doped with either 5-doxyl phosphatidylcholine, 10-doxyl phosphatidylcholine, or phosphatidyl-tempo-choline, quenching of acrylodan fluorescence was observed upon binding. Using the parallax method of London [Chattopadhyay, A., and London, E. (1987) *Biochemistry* 26, 39–45], the acrylodan ring is calculated to be 8.1 ± 2.5 Å from the center of the lipid bilayer. Modeling the acrylodan-cysteine residue as an extended chain suggests that the backbone of the loop does not penetrate into the lipid bilayer but interacts with the headgroups, i.e., the choline. These results demonstrate that cholesterol oxidase interacts directly with the lipid bilayer and sits on the surface of the membrane.

Cholesterol oxidase catalyzes the conversion of cholesterol to cholest-4-en-3-one when cholesterol is presented in the lipid phase as part of a lipid bilayer or in the aggregated form as detergent micelles. It is a bacterial enzyme secreted by *Streptomyces* and *Brevibacteria*, as well as other gram-positive bacteria. The bacteria produce cholesterol oxidase to utilize cholesterol as a source of carbon. The enzyme is used clinically to determine serum cholesterol concentrations and is being developed as an insecticide against the *Coleoptera* family (3, 4).

It is clear from a kinetic standpoint that cholesterol oxidase must associate with the lipid bilayer before binding substrate (5). That is, the enzyme does not bind cholesterol that has desorbed from the membrane and is free in solution. The maximum initial rate of turnover, i.e., when 100% of the enzyme is bound to a lipid vesicle, is 24 s^{-1} (5). In comparison, the rate of cholesterol desorption from 100-nm vesicles in the absence of enzyme is approximately $2 \times 10^{-5} \text{ s}^{-1}$ (6, 7). Thus, it is of interest to characterize the nature of the enzyme–lipid complex and to determine what types of molecular interactions are responsible for binding.

The dissociation constant of cholesterol oxidase for lipid vesicles may be measured using the change in fluorescence observed upon binding. We have constructed a single-cysteine mutant of cholesterol oxidase to specifically acrylodan label the enzyme. Use of this mutant facilitates the measurement of cholesterol oxidase binding to lipid vesicles under various conditions. In addition, the acrylodan fluorophore was used to probe the depth of protein insertion into the membrane by employing the parallax method of Chattopadhyay and London (8).

EXPERIMENTAL PROCEDURES

Materials. Cholest-4-en-3-one and cholesterol were purchased from Sigma Chemical Company (St. Louis, MO). Lipids were purchased from Avanti Polar Lipids (Alabaster, AL). The acrylodan and TCEP¹ were purchased from

[†] This work was supported by a grant from the NIH (HL53306, N.S.) and the American Heart Association (N.S.). The Center for Analysis and Synthesis of Macromolecules (CASM) at Stony Brook is supported by NIH Grant RR02427 and the Center for Biotechnology. Centrifuges and a fluorimeter were purchased with support from the NSF (CHE9808439 and CHE 9709164).

[‡] These authors contributed equally to this work.

* To whom correspondence should be addressed. Telephone: (631) 632-7952. Fax: (631) 632-5731. E-mail: nicole.sampson@sunysb.edu.

¹ Abbreviations: HPLC, high-pressure liquid chromatography; TCEP, tris-(2-carboxyethyl)phosphine; IPTG, isopropyl β -D-thiogalactoside; WT, wild type; LB, Luria broth; Tris-HCl, tris(hydroxymethyl)aminomethane hydrochloride; EDTA, ethylenediaminetetraacetate; SDS-PAGE, sodium dodecyl sulfate–polyacrylamide gel electrophoresis; DEAE, diethylaminoethyl; FPLC, fast protein liquid chromatography; M81C-Ad, C57S/M81C cholesterol oxidase labeled with acrylodan at C81; POPC, 1-palmitoyl-2-oleoyl-*sn*-glycero-3-phosphatidylcholine; POPS, 1-palmitoyl-2-oleoyl-*sn*-glycero-3-phosphatidylserine; DHEA, dehydroepiandrosterone (3 β -hydroxy-androst-5-en-17-one); ePC, egg phosphatidylcholine; 5-doxyl-PC, 1-palmitoyl-2-(5-doxyl)-stearoyl-*sn*-glycero-3-phosphocholine; 10-doxyl-PC, 1-palmitoyl-2-(10-doxyl)-stearoyl-*sn*-glycero-3-phosphocholine; tempocholine, 4-(*N,N*-dimethyl-*N*-(2-hydroxy-ethyl))ammonium-2,2,6,6-tetramethylpiperidine-1-oxyl; tempo-PC, 1-palmitoyl-2-oleoyl-*sn*-glycero-3-phosphotempocholeline; X_q , mole fraction of spin-labeled quencher.

Molecular Probes (Eugene, OR). The plasmid for heterologous expression of *Brevibacterium* cholesterol oxidase, pBCO1 has been previously described (9). Restriction endonucleases were purchased from New England Biolabs (Beverly, MA). Oligonucleotides were purchased from IDT, Inc. (Coralville, IA). Unless otherwise specified, all chemicals and solvents, of reagent or HPLC grade, were supplied by Fisher Scientific (Pittsburgh, PA). Water for assays and chromatography was distilled, followed by passage through a Barnstead NANOpure filtration system to give a resistivity better than 18 M Ω .

General Methods. Vesicles were prepared with an extruder from Lipex Biomembranes Inc. (Vancouver, BC, Canada). A Shimadzu UV2101 PC Spectrophotometer was used for assays. Fluorescence measurements were taken on a Spex Fluorolog 3-21 fluorimeter. Restriction digests and ligations were performed according to procedures described in Sambrook et al. (10). The buffers used were A: 50 mM sodium phosphate, pH 7.0; B: 50 mM sodium phosphate, pH 7.0, 0.025% Triton X-100; C: 50 mM sodium phosphate, pH 7.0, 1 mM TCEP.

Construction of pBCO5, C57S/M81C Mutant. The C57S² mutation was introduced into the pBCO1 vector (9) using the Sculptor In vitro Mutagenesis system (Amersham, Arlington Heights, IL) following the method of Eckstein (11, 12) as modified by Amersham. The primer used was 5'-TTGAGCATCCCGGAGAAGATCTT-3'. In addition, DNA Klenow polymerase was substituted for T7 DNA polymerase, and slow annealing conditions were used (70 °C for 20 min, 70–37 °C over 30 min). The second mutation, M81C, was incorporated using the QuickChange Site-Directed Mutagenesis kit (Stratagene, La Jolla, CA). The primers used were 5'-GTCAGCAACTTCTGCGGCTTCG-GCATC-3' and 5'-GATGCCGAAGCCGCAGAAGTTGCT-GAC-3'. The sequence was verified by CircumVent Thermal-Cycle sequencing using the manufacturer's protocol (New England Biolabs, Beverly, MA).

Purification of Wild-Type and C57S/M81C Cholesterol Oxidases. Wild-type cholesterol oxidase was purified as previously described (9). Cell paste of *Escherichia coli* BL21(DE3)plysS-(pBCO5) obtained from LB/kanamycin (30 μ g/mL) medium [grown at 37 °C for 10 h after addition of IPTG (1 mM) at A_{600} = 0.6] was resuspended in 50 mM Tris-HCl, 1 mM EDTA, and 1 mM TCEP, pH 7.0 (10 mL), and lysed by French press at 18 000 psi. All subsequent purification steps were performed at 4 °C and with 1 mM TCEP in the buffer. Cell debris was removed by centrifugation at 135 000g for 30 min. The supernatant was loaded onto a column of DEAE-cellulose (30 mm \times 15 cm, DE-52, Whatman) preequilibrated with buffer C. Protein was eluted with buffer C (80 mL, 10-mL fractions). Fractions containing cholesterol oxidase were concentrated by (NH₄)₂SO₄ precipitation (2.5 M final concentration). The pellet was redissolved in buffer C (1 mL), and (NH₄)₂SO₄ was added slowly to a final concentration of 2 M. The precipitate that formed was removed by centrifugation after 30 min, and the

cholesterol oxidase was allowed to crystallize over 2 days. The microcrystalline protein was collected by centrifugation, and the pellet of cholesterol oxidase was dissolved in buffer C and ultrafiltered (YM30 membrane, Amicon, Inc., Danvers, MA) into buffer C. Protein concentrations were determined by UV absorbance using ϵ_{280} = 72 774 M⁻¹ cm⁻¹ [calculated from the molar extinction coefficients of tryptophan and tyrosine (13)].

Construction of M81C-Ad Cholesterol Oxidase. The C57S/M81C mutant was stored in buffer C. Before labeling with acrylodan, TCEP was removed by ultrafiltration (YM30, Amicon, Inc., Danvers, MA) into deoxygenated buffer A (3 \times 1:50 dilution). Labeling was performed by adding 4 equiv of the probe as an acetonitrile solution (1 mg/mL) to the protein (0.16 mg/mL) with stirring at 4 °C for 4 h. The unreacted probe was removed by microdialysis (6000–8000 NMWCO, Spectrapor) against buffer A. The probe–protein ratio was determined by measuring the protein concentration with a Bradford assay (14) and the UV absorption of the probe (ϵ_{340} = 20 000 M⁻¹ cm⁻¹) (15). The labeled protein was stored at 4 °C in the dark.

Synthesis of Lipid Vesicles. Medium, 100-nm unilamellar vesicles were made from mixtures of lipids by extrusion (16). Lipids (10 μ mol) were mixed as CHCl₃ solutions in a round-bottomed flask, dried as a thin film under reduced pressure in a rotary evaporator for 20 min, and evacuated under high vacuum for 2 h. The lipid was resuspended in 1 mL of buffer A with vortexing. Five freeze–thaw cycles, at –80 °C and 37 °C, followed by 10 extrusion cycles through two stacked 100-nm filters (Costar, Cambridge, MA) using a nitrogen gas pressure of 350–400 psi, provided a homogeneous batch of vesicles. Phospholipid concentrations of vesicle solutions were measured using the Stewart assay (17) except when they contained nitroxide spin labels. The spin-labeled vesicles concentrations were determined by adding ¹⁴C-POPC to the initial lipid solution and using the specific activity to determine the final vesicle concentration. Cholesterol concentrations were measured by lysing vesicles with 0.1% Triton X-100 and using cholesterol oxidase to quantitate total cholesterol concentration as described below.

Activity Assay of Cholesterol Oxidase. The activity of wild-type cholesterol oxidase was measured by following the appearance of conjugated enone at 240 nm [ϵ_{240} = 12 100 M⁻¹ cm⁻¹ (18)]. When cholesterol was used as a substrate, it was added as a propan-2-ol solution to buffer B or as phospholipid vesicles to buffer A at 37 °C. When propan-2-ol was used, the final assay mixtures were 2% propan-2-ol. Dilute enzyme stock solutions contained 200 μ g/mL BSA. Assays with cholesterol in buffer B contained 200 μ g/mL BSA.

Fluorescence Binding Measurements. Binding of cholesterol oxidase to vesicles was assayed through the change in tryptophan or acrylodan fluorescence. All binding assays were conducted in buffer A at 20 °C. The instrument was operated in the ratio-recording mode. One-centimeter path length cuvettes were used. Samples were stirred during the assay to prevent the settling of the protein. The cuvettes were washed with nitric acid before each assay. For the intrinsic tryptophan fluorescence studies, 320-nm cut-on filters were placed before the emission monochromator to eliminate any contribution from scattered light. For the acrylodan fluores-

² This numbering refers to the X-ray crystal structure system for numbering amino acid residues (1). Numbering begins at the N-terminus of the processed *Brevibacterium* enzyme. Residue 57 and residues 73–86 are encoded by codons 102 and 118–131, respectively, in the *Brevibacterium* gene (2).

cence studies, 420-nm cut-on filters were used to eliminate any contribution from scattered light.

Tryptophan was excited at 280 nm, and the spectrum was acquired from 310 to 450 nm with a 1-nm excitation slit and a 3-nm emission slit. Acrylodan was excited at 360 nm, and the spectrum was acquired from 420 to 600 nm with a 1-nm excitation slit and a 3-nm emission slit. Sample signals were corrected for light fluctuations by simultaneously monitoring the exciting light on a reference photomultiplier. Protein (5–10 $\mu\text{g/mL}$) was titrated with increasing amounts of lipid vesicles (0–150 μL of a 3 mM stock solution) to a final concentration of 700 μM with constant stirring. Emission was corrected for any background signal by performing a titration in the absence of protein.

Binding constants were analyzed by first correcting spectra for dilution and background signal. The spectra were integrated and normalized to their value in the absence of added lipid. The binding isotherm was fitted to eq 1 using KaleidaGraph software (Synergy Software, Reading, PA):

$$\Delta F = (\Delta F_{\max} [L]) / ([L] + K_D) \quad (1)$$

[L], monomeric lipid concentration; K_D , dissociation constant; ΔF , change in fluorescence intensity; ΔF_{\max} , maximum change in fluorescence intensity.

Parallax Method of Depth-Dependent Fluorescence Quenching. Fluorescence quenching data for acrylodan-labeled cholesterol oxidase in the membrane-bound state was analyzed according to Chattopadhyay and London (8). The integrated fluorescence intensity for acrylodan upon excitation at 360 nm in the presence of the shallow quencher (tempo-PC or 5-doxyl-PC) was compared with the fluorescence intensity in the presence of the more deeply located quencher (5-doxyl-PC or 10-doxyl-PC). The fluorescence intensity was measured as a function of lipid concentration and fit to eq 1 above. The calculated ΔF_{\max} for each quencher, i.e., for 100% of enzyme bound to the vesicle, was used for F_1 and F_2 . The data were analyzed according to the following equations:

$$Z_{1F} = [(1/(-\pi C)) \ln(F_1/F_2) - 2L_{21}^2] / 2L_{21} \quad (2)$$

$$Z_{CF} = Z_{1F} + L_{C1} \quad (3)$$

where Z_{1F} is the distance from the fluorophore to the shallow quencher, C is the concentration of quencher within the bilayer, F_1 is the fluorescence intensity in the presence of the shallow quencher, F_2 is the fluorescence intensity in the presence of the deep quencher, L_{21} is the distance from shallow to deep quencher, L_{C1} is the distance from the center of the bilayer to the shallow quencher, L_{C2} is the distance from the center of the bilayer to the deep quencher, and Z_{CF} is the distance from the center of the bilayer to the fluorophore. F_1 and F_2 values are the average values of three independent experiments.

RESULTS

Kinetic Activity. Because saturating concentrations of cholesterol cannot be obtained in the detergent micelle conditions, the specific activity was measured at 50 μM cholesterol in 0.025% Triton X-100 at 37 °C at pH 7.0. For

Table 1: Dissociation Constants for Binding to 100-nm Vesicles

pH/lipid	K_D (μM)		
	M81C-Ad	Trp	M81C-Ad
	ePC		ePC/POPS (8:2)
6	979 \pm 15	nm ^a	nm ^a
7	223 \pm 22	48 \pm 7	200 \pm 58
8	240 \pm 17	nm	nm
9	110 \pm 33	nm	233 \pm 33

^a Not measured.

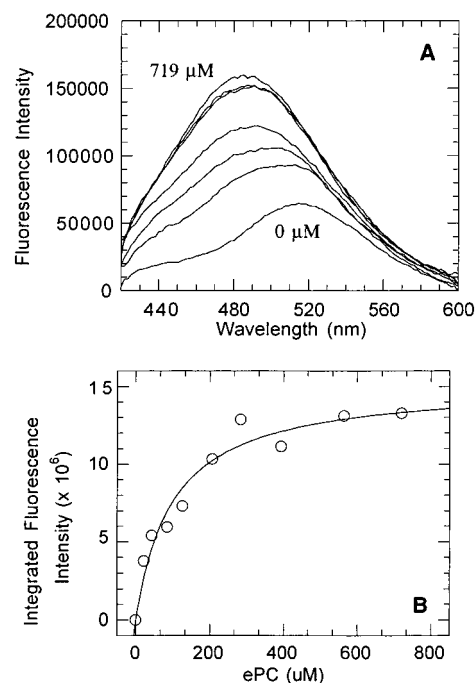


FIGURE 1: (A) Shift in emission spectra of M81C-Ad upon addition of ePC vesicles with excitation at 360 nm. (B) Representative binding isotherm of M81C-Ad upon addition of ePC vesicles.

wild-type *Brevibacterium* cholesterol oxidase (choB), it was 0.27 $\mu\text{mol mg}^{-1} \text{s}^{-1}$ and for M81C-Ad, it was 0.80 $\mu\text{mol mg}^{-1} \text{s}^{-1}$.

The kinetic activity with 100 nm ePC/cholesterol (1:1) vesicles was measured at 37 °C, pH 7.0. The $K_d(\text{app})$ for binding of wild-type choB to vesicles was 300 \pm 77 μM , and the initial velocity at saturation (v_i) was 7.6 \pm 0.8 s^{-1} . The $K_d(\text{app})$ for M81C-Ad was 13 \pm 1 μM , and the v_i was 16.3 \pm 0.1 s^{-1} .

Intrinsic Fluorescence Measurements using Wild-Type choB. The change in the intrinsic tryptophan fluorescence emission upon binding of wild-type choB to lipid vesicles was measured and fit to a binding isotherm (Table 1). The tryptophan emission using wild-type choB increased upon binding to lipid, consistent with a change from hydrophilic to hydrophobic environment. However, the emission maximum at 345 nm did not shift upon binding.

Characterization of Binding using the M81C-Ad Mutant. The probe–protein ratio of M81C-Ad was 0.37. The change in acrylodan fluorescence emission upon binding to lipid vesicles was measured and fit to a binding isotherm (Table 1 and Figure 1). The fluorescence emission increased and exhibited a blue shift in the emission maximum from 515 to 470 nm. The same mutant was used to determine the effect of pH (Table 1), lipid charge (Table 1), and ionic strength

Table 2: Dissociation Constants for M81C-Ad Binding to EPC and EPC/POPS (8:2) 100-nm Vesicles at Increasing Ionic Strength

[NaCl]	K_D (μ M)	
	ePC	ePC/POPS (8:2)
0	223 \pm 22	200 \pm 58
50	163 \pm 17	nm ^a
100	213 \pm 14	nm
500	142 \pm 25	220 \pm 90

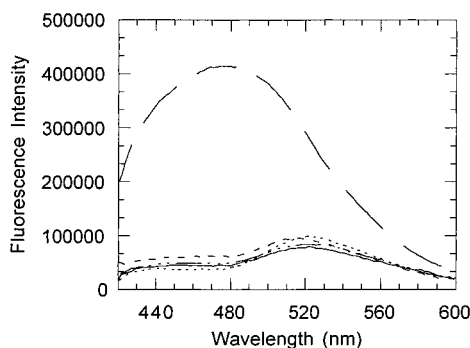
^a Not measured.

FIGURE 2: Quenched emission spectra of M81C-Ad upon binding to lipid vesicles: ePC (—); ePC/5-doxyl-PC, 35:65 (---); ePC/5-doxyl-PC, 50:50 (- - -); ePC/10-doxyl-PC, 35:65 (—); and ePC/10-doxyl-PC, 50:50 (- - -) vesicles. Each spectrum was acquired at a concentration of lipid at which 90% of the protein was bound to the vesicles. In the quenched spectra, the emission maximum at 520 nm is due to the 10% cholesterol oxidase that is still free in solution.

(Table 2) on binding. The binding affinity of M81C-Ad for lipids with a zwitterionic headgroup (POPC) was the same as the affinity in the presence of negatively charged lipid (POPS). Changes in ionic strength of the buffer medium did not have a significant effect on binding. Binding was also independent of pH until pH 6. At this pH, the enzyme begins to irreversibly denature.

Fluorescence with Nitroxide Spin-Label Quenchers. The acrylodan fluorescence emission was measured in the presence of three nitroxide quenchers in the lipid membrane: 5-doxyl-PC, 10-doxyl-PC, and tempo-PC. The binding affinity of the enzyme for the lipid vesicles did not change significantly as the mole fraction of quencher was varied. The K_d of cholesterol oxidase for ePC/5-doxyl-PC at a mole fraction of quencher (X_q) = 0.35 and 0.5 was 130 \pm 34 and 80 \pm 18 μ M, respectively, and for ePC/10-doxyl-PC at X_q = 0.35 and 0.5 was 220 \pm 3 and 110 \pm 8 μ M. The magnitude of quenching was measured at saturating concentrations of lipid vesicles as a function of mole fraction quencher. All three nitroxides quench the acrylodan fluorescence. The quenching is dependent on the mole fraction of quencher in the membrane until X_q = 0.35. Above X_q = 0.35, quenching was maximized (Figure 2), and therefore, quantitative parallax depths were measured with X_q = 0.5.

Parallax Depth Measurement. The magnitude of quenching was measured for vesicles containing each of the three nitroxide quenchers. For each pairwise combination, a preliminary depth calculation was performed. They all indicated that the acrylodan fluorophore of M81C-Ad was inserted in the membrane at a depth between the 5-doxyl-PC and the 10-doxyl-PC based on the ladder of London (8, 19) (Figure 4). Thus, this pair was used for quantitative

determination of the depth in three independent determinations at X_q = 0.5. A depth value (Z_{CF}) of 8.1 ± 2.5 Å (Figure 4) from the center of the bilayer (6.9 Å from the hydrophobic/hydrophilic interface of the membrane) was calculated from $F_{5\text{-doxyl}}/F_{10\text{-doxyl}} = 1.42 \pm 0.44$ according to eqs 2 and 3, using the values of $C = X_q/70$ Å², $L_{21} = 4.5$ Å, $L_{C1} = 12.15$ Å, and $L_{C2} = 7.65$ Å as given by London (8, 19). $F_{5\text{-doxyl}}/F_{ePC} = 0.25$ and $F_{10\text{-doxyl}}/F_{ePC} = 0.18$. F_{ePC} , $F_{5\text{-doxyl}}$, and $F_{10\text{-doxyl}}$ were calculated from the binding isotherms of M81C-Ad measured for vesicles containing the respective quenchers and ePC. The values of F_{ePC} , $F_{5\text{-doxyl}}$, and $F_{10\text{-doxyl}}$ correspond to the quenching observed at saturation of binding as calculated from fitting to eq 1.

DISCUSSION

Cholesterol oxidase is a member of a class of enzymes that are water-soluble and not permanently membrane-bound, yet whose substrates are part of the cell membrane. Other enzymes in this class are the lipases (20, 21), phospholipases (22, 23), fatty acid binding proteins (24–27), cholesterol esterases (28), cutinase (29), and some steroid dehydrogenases (30). To remain water-soluble, these catalysts must protect their hydrophobic binding cavities from the aqueous solvent until substrate is bound. The amphipathic lids of lipases (20) and cytosolic phospholipase A₂ (23) represent one structural motif for enzymes that hydrolyze highly hydrophobic substrates yet are soluble in the aqueous milieu. Secreted phospholipase A₂ and cholesterol esterase utilize two different motifs. The binding site of cholesterol esterase is a deep hydrophobic gorge that is formed by dimerization of the protein. The X-ray crystal structures suggest that in the absence of substrate the hydrophobic surface is protected from solvent by slight rotation of the monomers with respect to one another, i.e., a quarternary structure change (28). The active site of secreted phospholipase A₂ is not protected by a lid or protein interface. Instead, small adjustments in the position of aromatic side chains in the active site occur upon substrate binding (22). In addition, binding to the interface stabilizes the conformation of the N-terminal residues and the active site residues (31). Hence, the most polar phospholipids require minor structural changes as compared to the very hydrophobic cholesteryl fatty acid esters. Triacylglycerides are of intermediate hydrophobicity, requiring moderate conformational changes, i.e., active-site lids. It has been proposed that the cytosolic phospholipase A₂'s have a deeper cleft than the secreted enzymes to confer substrate specificity for arachidonyl phospholipids (23). Thus, the enzyme has a deep cleft for binding the fatty ester carbon tail. These examples suggest that the hydrophobicity of the substrate and the level of specificity required dictate the molecular architecture required for its binding (32).

Both the hydrophobicity of cholesterol and the specificity of cholesterol oxidase suggest that cholesterol oxidase utilizes an active-site lid in a manner similar to the lipases. Our hypotheses about mode of action are based on X-ray crystal structures and kinetic information. Two X-ray crystal structures have been solved of the *Brevibacterium* cholesterol oxidase. One of the native enzyme (1) and one with dehydroepiandrosterone, a substrate analogue, bound (33). In addition, we have recently solved the *Streptomyces* native cholesterol oxidase structure (34). The steroid binding site whether filled with water or with steroid is completely

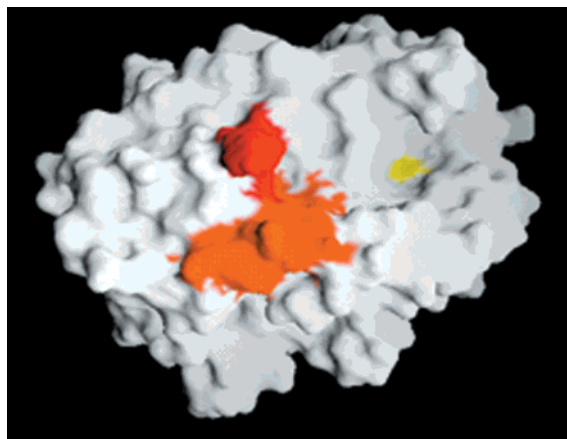


FIGURE 3: GRASP (37) model of the *Brevibacterium* structure demonstrating that the active site is sequestered from bulk solvent by the protein. The proposed conformationally flexible loops are shown in red and gold, dehydroepiandrosterone is in blue (but not visible), and FAD is in yellow.

sequestered from bulk solvent. Clearly, during the binding process a conformational change must occur that exposes the binding cavity to lipid bilayer or detergent micelle. In the dehydroepiandrosterone-bound structure, the C17-truncated steroid completely fills the binding cavity. It is not clear what the conformation of the protein will be with cholesterol bound, as cholesterol has an 8-carbon tail, nor is the structure of the complex of protein and lipid membrane known.

Two surface loops (73–86, 432–438) appear to cap the active site (Figure 3). Although the conformation of the “open” enzyme is not known, we postulated that one or both of these loops open to form a hydrophobic pathway between the membrane and the active site. Previously, we had shown that the loop containing residues 73–86 is important for binding substrate and for substrate specificity (5). Although deletion of the loop did not reduce the binding affinity of cholesterol oxidase for the membrane, it did significantly reduce the kinetic activity of the enzyme on vesicle substrates. The outside faces of the loops are hydrophilic, and the inside faces consist of hydrophobic amino acids. Thus the loops form a hydrophobic pathway. This pathway would lower the activation barrier for cholesterol movement out of the bilayer. Upon binding, the four rings of the sterol are completely buried in the substrate-binding site. With deletion of the loop, the pathway from lipid vesicle to enzyme active site becomes exposed to water and raises the kinetic barrier to binding substrate. In the dehydroepiandrosterone structures, the loops can close over the substrate analogue and bury it because dehydroepiandrosterone has a ketone at C₁₇. Presumably, when cholesterol is bound, the 8-carbon “tail” sticks out of the binding site and packs with the open loops. Whether or not the C₁₇-tail is left in the membrane depends on the conformation of the two surface loops. Upon deletion of the large loop the enzyme becomes less specific for cholesterol and more specific for dehydroepiandrosterone with respect to wild type. These results are consistent with a model in which the loop packs with the cholesterol tail.

To pinpoint the level of membrane interaction of cholesterol oxidase with the lipid bilayer, we have used steady-state fluorescence to study the binding of the enzyme to the membrane under various conditions. Although intrinsic

tryptophan fluorescence may be used to measure binding, we used a single cysteine mutant of the *Brevibacterium* enzyme (9). In these experiments, we chose the *Brevibacterium* enzyme because it only had one other cysteine present that we were able to mutate to a serine without any change in activity. We introduced a cysteine into the active site loop (residues 73–86) at position 81 that is a methionine in the wild-type enzyme.² As discussed above, the X-ray crystal structures (1, 33) suggested that this face of the enzyme must be oriented toward the membrane. Moreover, the kinetic results (5) indicated that interaction of the loop with the membrane is kinetically important, although it does not contribute significantly to the binding affinity of the enzyme for the membrane. Hence, we reasoned that substitution of a methionine with an acrylodan should not significantly perturb the binding affinity of the enzyme for the membrane.

The loop-cysteine mutant was then labeled with acrylodan, an environment-sensitive fluorescence probe. We observed fluorescence increasing and shifting toward blue emission upon binding to lipid vesicles, consistent with a change into a more hydrophobic, i.e., lipid, environment. The binding affinity for the membrane was only decreased 4-fold relative to the wild-type cholesterol oxidase. The kinetic activity with cholesterol was improved suggesting that the acrylodan and by inference the methionine is important for binding substrate in the active site. These observations are consistent with the aforementioned loop deletion experiments (5).

We used this acrylodan-labeled cholesterol oxidase to explore the dependence of binding on pH, ionic strength, and headgroup charge. Between pH 7 and 10, there is no significant change in binding affinity. Incorporation of anionic lipids (phosphatidylserine) into the vesicles did not increase the binding affinity, nor did altering the ionic strength. These experiments all suggest that the protein–membrane interactions are primarily driven by hydrophobic effects not ionic effects. The insensitivity of enzyme binding to electrostatics and pH may reflect the scavenger function of the enzyme. In bacteria, cholesterol oxidase is part of an operon for utilizing steroids as a carbon source. Presumably, the more general the binding characteristics, the wider variety of membranes that may be used as fuel.

We further explored the interaction of the acrylodan-labeled enzyme with membranes using vesicles doped with either 5-doxyl phosphatidylcholine, 10-doxyl phosphatidylcholine, or tempo-labeled phosphatidylcholine. With each of these membrane spin-labels, we observe a quenching of acrylodan fluorescence upon binding of the enzyme to the vesicle. Quenching by spin-labels is distance-dependent and decreases with r^6 . The quenching we observe upon incorporation of spin-label into the vesicles confirms that the fluorescence changes detected upon titration of enzyme with vesicles are due to binding of the enzyme to the membrane.

We then applied the parallax method of London (35) to our acrylodan-cholesterol oxidase system. We calculated the distance between the fluorophore and the center of the membrane using pairs of quenchers. Calculations with all three pairs gave the same qualitative results and indicated that the fluorophore sits in the membrane between the 5-doxyl-PC and the 10-doxyl-PC. Hence, we used this pair for quantitative calculations and subsequent modeling. Moreover, calculation of the same approximate depth with two different pairs of quenchers present at different depths

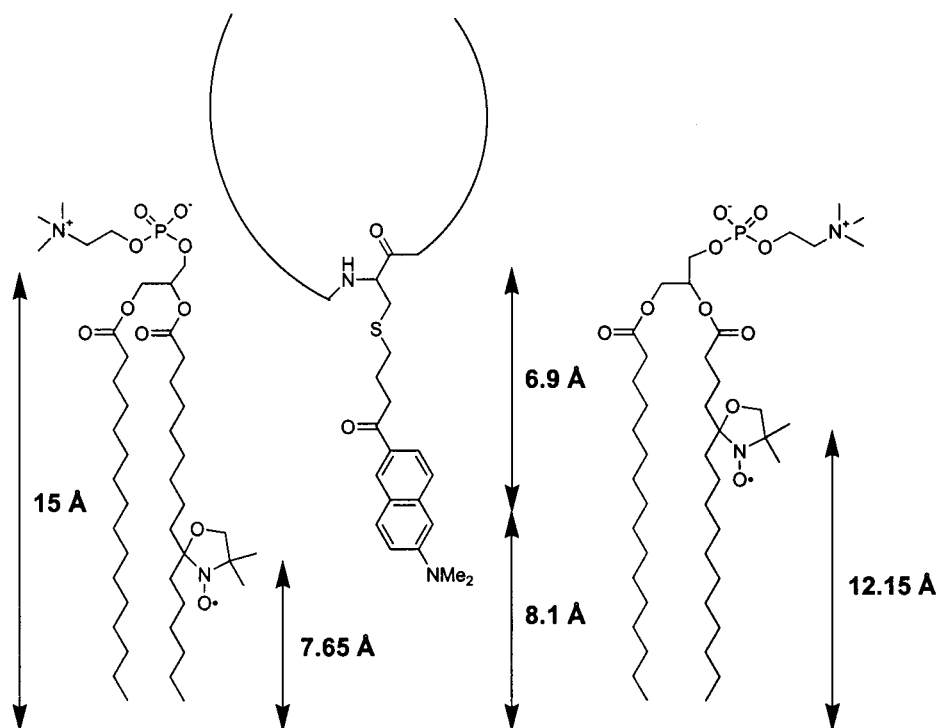


FIGURE 4: Model of membrane-cholesterol oxidase interactions based on parallax measurements.

means that the fluorophore occupies one average position within the membrane. That is, there are not two populations of fluorophore at different membrane depths.

With the 5-doxyl/10-doxyl pair, we calculated that the acrylodan ring is 8.1 Å from the center of the lipid bilayer. The dissociation constant of cholesterol oxidase for the membrane is not significantly perturbed by incorporation of spin-label quenchers into the membrane. The insensitivity of binding implies that the depth of fluorophore insertion is also insensitive to quencher in the membrane, and thus, the measured depth to an ePC vesicle would be the same. In addition, we considered the possibility that the fluorophore was sufficiently deep in the membrane that quenching could also be a result of trans leaflet quenching by the 10-doxyl-PC. The estimated distance ($Z_{CF} + L_{C2}$) from trans 10-doxyl-PC to the acrylodan label is 15.8 Å. London and Feigenson (36) calculate that for doxyl quenchers the critical separation distance between quencher and fluorophore, R_C , is in the range 10–11 Å. Only if the R_C is larger than the actual distance between the quencher and the fluorophore, must trans leaflet quenching be considered. Thus, trans bilayer quenching by 10-doxyl-PC is not important for our measurements.

To estimate the position of the remainder of cholesterol oxidase with respect to the membrane, we modeled the linker as an extended chain because this presents the most conservative model of the enzyme-membrane interactions. Our modeling is limited by the degrees of freedom about the acrylodan-cysteine linker. This is a limitation of all currently available fluorescent protein-modification reagents. Modeling the acrylodan-cysteine residue as an extended chain suggests that the backbone of the loop does not penetrate into the lipid bilayer but interacts with the headgroups, i.e., the choline (Figure 4). These results support our model of cholesterol oxidase membrane docking and are consistent with previous mutagenesis experiments (5). That is, the

enzyme is on the surface of the membrane, and the amino acid side chains of the loop insert into the membrane to shield the cholesterol from the polar headgroups as it moves from the bilayer into the active site. We do not yet know the extent of the enzyme surface that is in contact with the membrane; however, from mutagenesis experiments, we know that the contact surface is composed of more than the loop itself. The insensitivity of binding constants to ionic strength, charge, and pH show that the binding affinity is driven by hydrophobic interactions not electrostatics.

We conclude that parallax measurements are an important tool for defining the structure of cholesterol oxidase at the membrane surface. We now know the position of the tip of loop with respect to the membrane. Further labeling studies are required to determine the orientation of the protein with respect to the membrane and the magnitude of the surface area that is in contact with the membrane.

ACKNOWLEDGMENT

We thank Prof. Erwin London for his helpful scientific advice.

REFERENCES

1. Vrielink, A., Lloyd, L. F., and Blow, D. M. (1991) *J. Mol. Biol.* 219, 533–554.
2. Ohta, T., Fujishiro, K., Yamaguchi, K., Tamura, Y., Aisaka, K., Uwajima, T., and Hasegawa, M. (1991) *Gene* 103, 93–96.
3. Purcell, J. P., Greenplate, J. T., Jennings, M. G., Ryerse, J. S., Pershing, J. C., Sims, S. R., Prinsen, M. J., Corbin, D. R., Tran, M., Sammons, R. D., and Stonard, R. J. (1993) *Biochem. Biophys. Res. Commun.* 196, 1406–1413.
4. Greenplate, J. T., Duck, N. B., Pershing, J. C., and Purcell, J. P. (1995) *Entomol. Exp. Appl.* 74, 253–258.
5. Sampson, N. S., Kass, I. J., and Ghoshroy, K. B. (1998) *Biochemistry* 37, 5770–5778.

6. Rodriguez, W. V., Wheeler, J. J., Klimuk, S. K., Kitson, C. N., and Hope, M. J. (1995) *Biochemistry* 34, 6208–6217.
7. McLean, L. R., and Phillips, M. C. (1981) *Biochemistry* 20, 2893–2900.
8. Chattopadhyay, A., and London, E. (1987) *Biochemistry* 26, 39–45.
9. Sampson, N. S., and Chen, X. C. (1998) *Prot. Exp. Purific.* 12, 347–352.
10. Sambrook, J., Fritsch, E. F., and Maniatis, T. (1989) *Molecular Cloning: A Laboratory Manual*, 2nd ed., Cold Spring Harbor Laboratory Press, Cold Spring Harbor, New York.
11. Nakamaye, K., and Eckstein, F. (1986) *Nucleic Acids Res.* 14, 9679–9698.
12. Sayers, J. R., Schmidt, W., and Eckstein, F. (1988) *Nucleic Acids Res.* 16, 791–802.
13. Fasman, G. D. (1992) *Practical Handbook of Biochemistry and Molecular Biology*, C. R. C. Press, Boca Raton, FL.
14. Bradford, M. M. (1976) *Anal. Biochem.* 72, 248–254.
15. Molecular Probes (Eugene, OR), personal communication.
16. Hope, M. J., Bally, M. B., Webb, G., and Cullis, P. R. (1985) *Biochim. Biophys. Acta* 812, 55–65.
17. Stewart, J. C. M. (1959) *Anal. Biochem.* 104, 10–14.
18. Smith, A. G., and Brooks, C. J. W. (1977) *Biochem. J.* 167, 121–129.
19. Abrams, F. S., Chattopadhyay, A., and London, E. (1992) *Biochemistry* 31, 5322–5327.
20. Cygler, M., and Schrag, J. D. (1997) *Methods Enzymol.* 284, 3–27.
21. Roussel, A., Canaan, S., Egloff, M.-P., Riviere, M., Dupuis, L., Verger, R., and Cambillau, C. (1999) *J. Biol. Chem.* 274, 16995–17002.
22. Scott, D. L., White, S. P., Otwinowski, Z., Yuan, W., Gelb, M. H., and Sigler, P. B. (1990) *Science* 250, 1541–1546.
23. Dessen, A., Tang, J., Schmidt, H., Stahl, M., Clark, J. D., Seehra, J., and Somers, W. S. (1999) *Cell* 97, 349–360.
24. Sacchettini, J. C., Gordon, J. I., and Banaszak, L. J. (1989) *J. Mol. Biol.* 208, 327–339.
25. Hodsdon, M. E., and Cistola, D. P. (1997) *Biochemistry* 36, 2278–2290.
26. Hodsdon, M. E., and Cistola, D. P. (1997) *Biochemistry* 36, 1450–1460.
27. Cistola, D. P., Kim, K., Rogl, H., and Frieden, C. (1996) *Biochemistry* 35, 7559–7565.
28. Ghosh, D., Wawrzak, Z., Pletnev, V. Z., Li, N., Kaiser, R., Pangborn, W., Jornvall, H., Erman, M., and Duax, W. L. (1995) *Structure* 3, 279–288.
29. Longhi, S., Czjzek, M., Lamzin, V., Nicolas, A., and Cambillau, C. (1997) *J. Mol. Biol.* 268, 779–799.
30. Duax, W. L., Griffin, J. F., and Ghosh, D. (1996) *Curr. Opin. Struct. Biol.* 6, 813–823.
31. van den Berg, B., Tessari, M., Boelens, R., Dijkman, R., de Haas, G. H., Kaptein, R., and Verheij, H. M. (1995) *Struct. Biol.* 2, 402–406.
32. Cambillau, C., Longhi, S., Nicolas, A., and Martinez, C. (1996) *Curr. Opin. Struct. Biol.* 6, 449–455.
33. Li, J., Vrielink, A., Brick, P., and Blow, D. M. (1993) *Biochemistry* 32, 11507–11515.
34. Yue, K., Kass, I. J., Sampson, N., and Vrielink, A. (1999) *Biochemistry* 38, 4277–4286.
35. Abrams, F. S., and London, E. (1992) *Biochemistry* 31, 5312–5322.
36. London, E., and Feigenson, G. W. (1981) *Biochemistry* 20, 1932–1938.
37. Nicholls, A., Sharp, K. A., and Honig, B. (1991) *Proteins* 11, 281–296.

BI001407J